JOURNAL OF CATALYSIS 135, 186–199 (1992)

Acidic Properties of Supported Niobium Oxide Catalysts: An Infrared Spectroscopy Investigation

J. DATKA,[1] A. M. TUREK,[1] J. M. JEHNG, AND I. E. WACHS[2]

Zettlemeyer Center for Surface Studies, Department of Chemical Engineering, Lehigh University, Bethlehem, Pennsylvania 18015

Received February 5, 1991; revised November 12, 1991

Chemisorption of pyridine was applied as a method for studying the acidic properties of niobium pentoxide supported on silica, magnesia, alumina, titania, and zirconia. The infrared spectra of adsorbed pyridine were used to evaluate the concentration and the relative strength of Brønsted and Lewis acid sites. Lewis acidity was found in all the supported niobium oxide systems, while Brønsted acid sites were only detected for niobia supported on the alumina and silica supports. The origin and characteristics of the surface acid sites present in supported niobium oxide catalysts are discussed in the present study. © 1992 Academic Press, Inc.

INTRODUCTION

Chemisorption of pyridine followed by IR studies is usually a useful probe for the presence and nature of surface Lewis acid and Brønsted acid sites on a catalyst surface (*1*). According to Knozinger (*2*), the vibrational modes of pyridine that are the most affected through such intermolecular interactions are the ring-stretching modes 19b and 8a (originally at 1439 and 1583 cm^{-1}, respectively (*3*)). These two modes are observed at 1440–1450 and 1580–1600 cm^{-1}, respectively, for hydrogen-bonded pyridine, at 1535–1550 and about 1640 cm^{-1} for pyridinium ion (PyH^+), and at 1440–1460 and 1600–1635 cm^{-1} for pyridine coordinatively bonded to Lewis acid sites (PyL). The hydrogen-bonded pyridine is only observed at low evacuation temperatures (below 473 K) (*4*).

The concentration of Brønsted and Lewis acid sites can be determined from the intensities of the PyH^+ and PyL bands and their extinction coefficients after saturation of all the surface acid sites by the method proposed by Hughes and White (*5*). Information on the strength of Brønsted and Lewis acid sites can be obtained from pyridine thermodesorption experiments and, in the case of Lewis acid sites, to some extent, from the position of the PyL band in the 1440–1460 cm^{-1} region since the frequency usually increases with the acid strength of the Lewis acid sites (*6–8*).

In the present investigation, pyridine adsorption studies were undertaken to learn more about the acidic properties of niobium oxide supported on SiO_2, Al_2O_3, MgO, TiO_2, and ZrO_2. Prior acidity studies of niobium oxide supported on Al_2O_3 and TiO_2 revealed that such catalysts can possess strong acid sites, but none of these studies employed pyridine adsorption as a probe and the molecular state of the supported niobium oxide phases was not known (*9–12*). Raman spectroscopy characterization (*13–15*) and EXAFS (*16–18*) studies of the supported niobium oxide catalysts demonstrated that, with the exception of the Nb_2O_5/SiO_2 system, the supported niobium oxide phases were present as a two-dimensional niobium oxide overlayer on the high-surface-area oxide supports. The weaker in-

[1] On leave from Faculty of Chemistry, Jagiellonian University, Cracow, Poland.

[2] To whom correspondence should be addressed.

0021-9517/92 $3.00

teraction between Nb_2O_5 and the SiO_2 surface resulted in the formation of a surface niobium oxide phase below 2 wt% Nb_2O_5/SiO_2 and the formation of bulk Nb_2O_5, in addition to the surface niobium oxide phase, at higher niobium oxide loadings (*15, 19*). The objective of this investigation is to determine the acidic properties of the niobium oxide overlayers as well as the influence of the different oxide substrates.

EXPERIMENTAL

The oxide supports employed in the present study are: MgO (Fluka, ~80 m^2/g; obtained from $Mg(OH)_2$ and calcined at 700°C for 2 h), Al_2O_3 (Harshaw, ~180 m^2/g after calcination at 500°C for 16 h), TiO_2 (Degussa, ~50 m^2/g after calcination at 450°C for 2 h), ZrO_2 (Degussa, ~39 m^2/g after calcination at 450°C for 2 h), and SiO_2 (Cab-O-Sil, ~275 m^2/g after calcination at 500°C for 16 h). Hydrated niobium pentoxide, $Nb_2O_5 \cdot nH_2O$, was provided by the Niobium Products Company (Pittsburgh, PA) with a minimum purity of 99.0%. The major impurities after calcining at 800°C are 0.02% Ta and 0.01% Cl. The TiO_2-, ZrO_2-, SiO_2-, and Al_2O_3-supported niobium oxide catalysts were prepared by the incipient-wetness impregnation method using niobium oxalate/oxalic acid aqueous solutions (aqueous preparation) (*13*). Niobium oxalate was supplied by Niobium Products Company with the following chemical analysis: 20.5% Nb_2O_5, 790 ppm Fe, 680 ppm Si, and 0.1% insolubles. The water-sensitive MgO support required the use of niobium ethoxide/propanol solutions, a nonaqueous preparation, under a nitrogen environment for the preparation of the Nb_2O_5/MgO catalysts. Niobium ethoxide (99.999% purity) was purchased from Johnson Matthey (Ward Hill, MA).

For the aqueous preparation method, the samples were initially dried at room temperature for 16 h, further dried at 110–120°C for 16 h, and calcined at 450°C (Nb_2O_5/TiO_2 and Nb_2O_5/ZrO_2) for 2 h and at 500°C (Nb_2O_5/Al_2O_3 and Nb_2O_5/SiO_2) for 16 h under flowing air. For the nonaqueous preparation method, the Nb_2O_5/MgO samples were initially dried at room temperature for 16 h, further dried at 110–120°C for 16 h under flowing N_2, and subsequently calcined at 500°C for 1 h under flowing N_2 followed by final calcination at 500°C for 1 h under flowing dry air.

The IR spectra were recorded on an Analect fX-6160 FTIR spectrometer with a resolution experimentally determined as better than 2 cm^{-1}. The catalysts were pressed into thin wafers (20–30 mg/cm^{-2}) and activated *in situ* in the IR cell (vacuum, 425°C, 1 h). The cell was cooled to 200°C and the IR spectrum was recorded. Pyridine was then introduced into the cell at 5 Torr and contacted with the catalyst for 30 s. Physically adsorbed pyridine was subsequently desorbed by maintaining the sample in vacuum for 15 min, and the IR pyridine adsorption spectrum was then recorded. The concentrations of Brønsted and Lewis acid sites were calculated from the intensities of PyH^+ and PyL bands and their extinction coefficients (the determination of the coefficients is described below). Pyridine thermodesorption experiments were also made in order to study the acid strength of the Lewis sites. Pyridine was desorbed by holding the catalyst at 350°C in vacuum for 15 min. The cell was then cooled to 200°C and the IR spectrum was again recorded. The PyL band intensity was measured and the A_{des}/A_0 ratio was calculated (A_0 and A_{des} are the intensities of PyL band before and after desorption, respectively). The value of A_{des}/A_0 represents the fraction of Lewis acid sites still containing adsorbed pyridine after the desorption at the "standard" conditions (350°C, 15 min) and is taken as a measure of the acid strength of the Lewis acid sites (*7*). For all the investigated catalysts the corresponding A_{des}/A_0 ratio for the PyH^+ band was found to equal 0.

The integrated extinction coefficient of the 1450 cm^{-1} PyL band was determined by experiments in which measured amounts of pyridine were adsorbed on an Al_2O_3 support

containing only Lewis acid sites (the PyH^+ band was not observed). The integrated intensity of the 1450 cm^{-1} band increased linearly with the amount of adsorbed pyridine. The slope of the line was taken as the extinction coefficient and the value of 1.11 cm μmol^{-1} was obtained for the 1450 cm^{-1} PyL band (*20*).

The integrated extinction coefficient of the 1540 cm^{-1} PyH^+ band was determined by adsorbing measured portions of pyridine on HY zeolite, Si/Al = 2.6, which was activated at 450°C under the conditions that prevented dehydroxylation (PyL band was absent). The value of 0.73 cm μmol^{-1} was obtained for the extinction coefficient of the 1540 cm^{-1} PyH^+ band.

RESULTS

Acidic properties of the oxide supports: Silica, magnesia, alumina, titania, zirconia, and niobia. The IR spectra of pyridine adsorbed on the oxide supports are presented in Figs. 1–5, and the Lewis acid site (LAS) and the Brønsted acid site (BAS) concentrations as well as the A_{des}/A_0 ratios for the 1450 cm^{-1} PyL band are tabulated in Table 1. Lewis acid sites are present on the alumina, niobia, titania, and zirconia supports, but not on the silica and magnesia supports. Brønsted acid sites are absent for all the oxide supports activated at 350°C, but niobia activated at 200°C does possess Brønsted acid sites (see Table 1). There are no Lewis or Brønsted acid sites detectable by pyridine chemisorption for niobia calcined at 500°C, but Lewis and Brønsted acid sites are detected on niobia samples activated at 200°C. These results are consistent with the previous determinations for pyridine chemisorbed on hydrated niobia at different temperatures reported by Tanabe and co-workers (*21*). The strength of the Lewis acid sites present on the pure oxide supports investigated in this study increases in the order Zr < Ti < Nb< Al and is reflected in the shift of the 1450 cm^{-1} PyL band position (see Fig. 6).

Acidic properties of niobia/silica. The IR

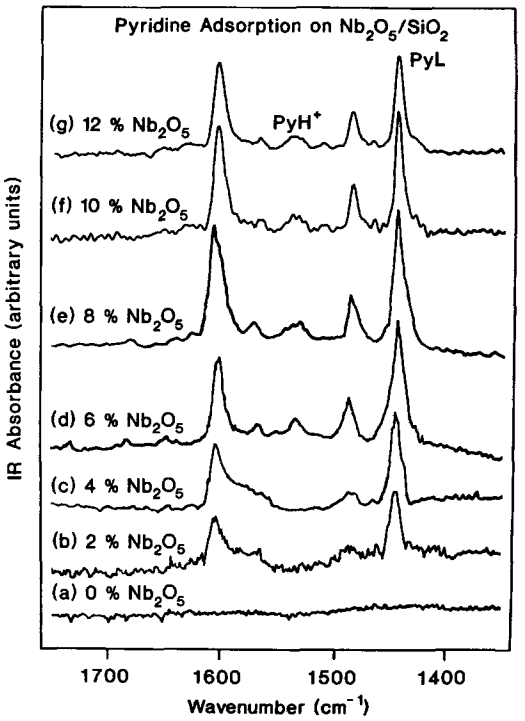

FIG. 1. Infrared spectra of pyridine adsorbed on Nb_2O_5/SiO_2 catalysts with niobia loading: (a) 0 wt%, (b) 2 wt%, (c) 4 wt%, (d) 6 wt%, (e) 8 wt%, (f) 10 wt%, (g) 12 wt%.

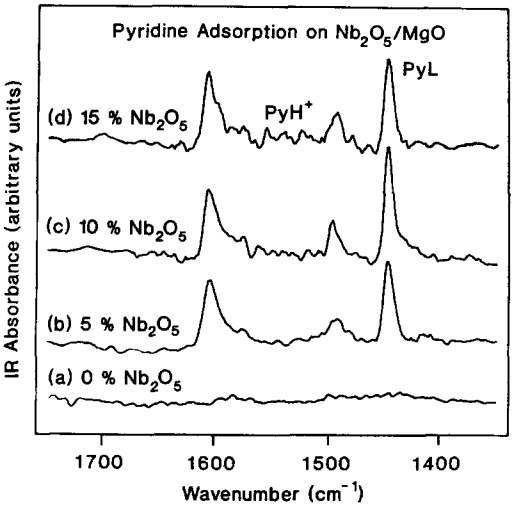

FIG. 2. Infrared spectra of pyridine adsorbed on Nb_2O_5/MgO catalysts with niobia loading: (a) 0 wt%, (b) 5 wt%, (c) 10 wt%, (d) 15 wt%.

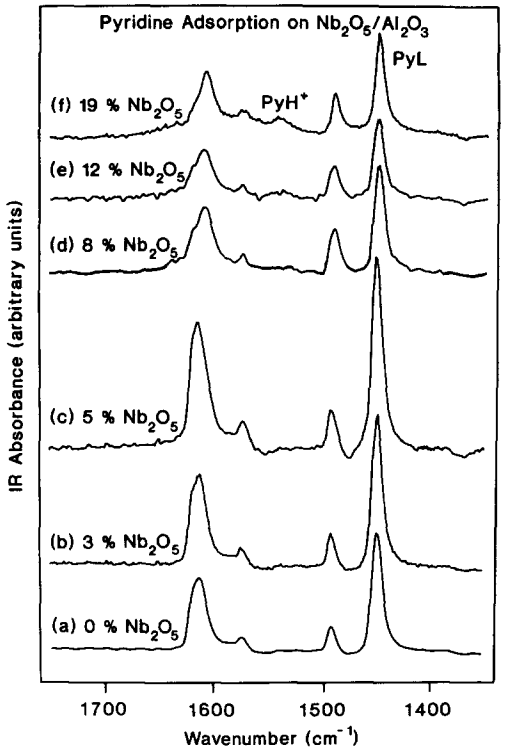

FIG. 3. Infrared spectra of pyridine adsorbed on Nb_2O_5/Al_2O_3 catalysts with niobia loading: (a) 0 wt%, (b) 3 wt%, (c) 5 wt%, (d) 8 wt%, (e) 12 wt%, (f) 19 wt%.

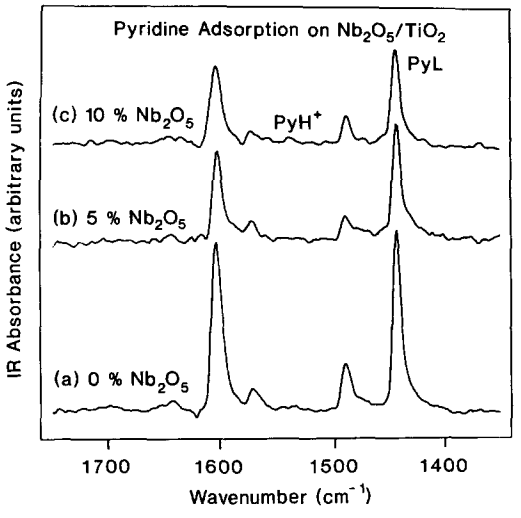

FIG. 4. Infrared spectra of pyridine adsorbed on Nb_2O_5/TiO_2 catalysts with niobia loading: (a) 0 wt%, (b) 5 wt%, (c) 10 wt%.

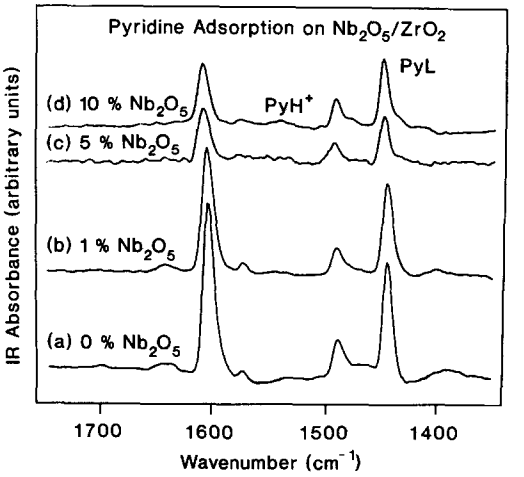

FIG. 5. Infrared spectra of pyridine adsorbed on Nb_2O_5/ZrO_2 catalysts with niobia loading: (a) 0 wt%, (b) 1 wt%, (c) 5 wt%, (d) 10 wt%.

TABLE 1

Acidic Properties of Supported Niobium Oxide Catalysts

Catalyst	Amount of LAS (μmol/g)	A_{des}/A_0	Amount of BAS (μmol/g)
Niobic acid (act. 200°C)	152	0.33	57
Niobic acid (cal. 500°C)	0	0	0
SiO_2	0	0	0
2% Nb_2O_5/SiO_2	22	0	0
4% Nb_2O_5/SiO_2	41	0	0
6% Nb_2O_5/SiO_2	60	0	20
8% Nb_2O_5/SiO_2	66	0.10	33
10% Nb_2O_5/SiO_2	56	0	21
12% Nb_2O_5/SiO_2	45	0	11
Al_2O_3	199	0.53	0
3% Nb_2O_5/Al_2O_3	221	0.54	0
5% Nb_2O_5/Al_2O_3	263	0.55	0
8% Nb_2O_5/Al_2O_3	184	0.50	10
12% Nb_2O_5/Al_2O_3	130	0.47	38
19% Nb_2O_5/Al_2O_3	154	0.38	54
TiO_2	126	0	0
5% Nb_2O_5/TiO_2	80	0	0
10% Nb_2O_5/TiO_2	70	0	5
MgO	0	0	0
5% Nb_2O_5/MgO	72	0	0
10% Nb_2O_5/MgO	96	0	0
15% Nb_2O_5/MgO	77	0	7
ZrO_2	73	0	0
1% Nb_2O_5/ZrO_2	57	0	0
5% Nb_2O_5/ZrO_2	29	0	0
10% Nb_2O_5/ZrO_2	42	0	4

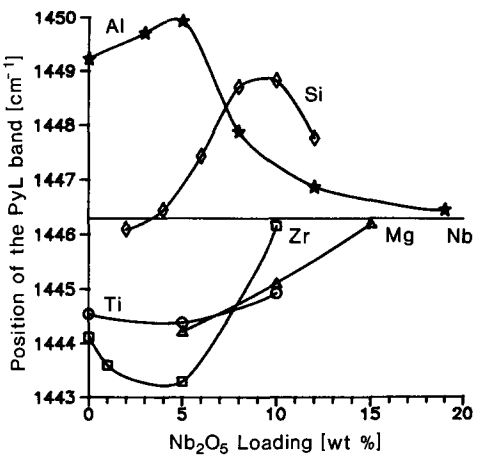

FIG. 6. Infrared absorption frequencies for the 1450 cm^{-1} PyL band as a function of the amount of deposited niobia. The horizontal line represents the position of the PyL band for bulk Nb_2O_5.

spectra of pyridine adsorbed on the niobia/silica catalysts are presented in Fig. 1. Silica itself shows neither Brønsted nor Lewis acid sites, but the addition of niobia to the SiO_2 surface creates Lewis acid sites, as well as Brønsted acid sites at higher loadings. The acid site concentrations (in micromoles per gram of sample) as a function of niobium oxide loadings are listed in Table 1 and plotted in Fig. 7. For low loadings of niobium oxide, the concentration of LAS increases linearly with the number of Nb atoms. Assuming that only Nb atoms are responsible for Lewis acid sites in this catalyst and comparing the amount of LAS determined spectroscopically with the amount of Nb atoms present in 1 g of a catalyst suggest that in the range from 2 to 6 wt% Nb_2O_5/SiO_2 the Lewis acid concentration is relatively stable and corresponds on average to ~14% of the total Nb atoms deposited on the silica support. Consequently, approximately 1 out of 7–8 Nb atoms contributes to the Lewis acidity detectable in the IR spectrum after chemisorption of pyridine. Such a low contribution of the Nb atoms to Lewis acidity at low loadings of niobia, when the dispersion of Nb_2O_5 is high, results from a relatively low concentration of the surface niobia species, which are successively and to a great extent replaced by particles of crystalline niobia with much inferior acidic properties. For higher loadings this ratio becomes much lower (changing from 1:11 for 8 wt% Nb_2O_5/SiO_2 to 1:20 for 12 wt% Nb_2O_5/SiO_2 because of the large Nb_2O_5 particles formed at these high loadings (*15*, *19*)). The only nonzero A_{des}/A_0 value (see Table 1 for pyridine thermodesorption data) found for the 8 wt% sample may be a result of a PyH^+ band integration error, which in this case allows an estimate of the amount of Lewis acid sites with an accuracy ±5 μmol/g.

The deposition of niobia on silica also creates Brønsted acid sites, which appear only at higher loadings (above 4 wt% Nb_2O_5/SiO_2; see Figs. 1 and 7). The amount of such Brønsted sites is relatively low: only 4.4% of all Nb atoms contributes to the Brønsted acidity for the 6 wt% Nb_2O_5/SiO_2 sample, 5.5% for the 8 wt% Nb_2O_5/SiO_2 sample, 2.8% for the 10 wt% Nb_2O_5/SiO_2 sample, and 1.2% for the 12 wt% Nb_2O_5/SiO_2 sample.

Acidic properties of niobia/magnesia.

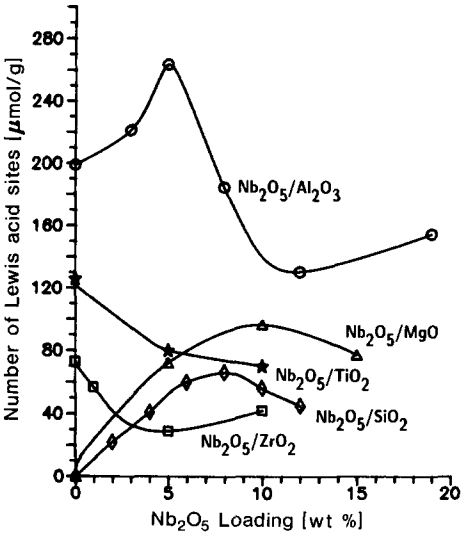

FIG. 7. Amount of Lewis acid sites as a function of the amount of deposited niobia.

The IR spectra of pyridine adsorbed on niobia/magnesia catalysts are presented in Fig. 2. The magnesia support does not reveal Brønsted or Lewis acid sites, but deposition of niobia on the MgO surface creates new Lewis acid sites, and does not produce Brønsted acid sites (see Figs. 2 and 7). The observed traces of BAS for 15 wt% Nb_2O_5/MgO are probably due to crystallites of niobia. The concentration and strength of Lewis acid sites are shown in Table 1. The amount of LAS created by the niobia addition corresponds to 19.1% of the Nb atoms deposited for the 5 wt% Nb_2O_5/MgO sample, to 12.8% for the 10 wt% Nb_2O_5/MgO sample, and to only 6.8% for the 15 wt% Nb_2O_5/MgO sample. In spite of the fact that in the case of niobia/magnesia catalysts a larger fraction of the Nb atoms contributes to Lewis acidity compared with niobia/silica catalysts, the acid strength of the former appears to be relatively low. This is reflected in the position of the 1450 cm^{-1} PyL band, which is a linear function of the amount of Nb atoms and attains a value characteristic of niobia (1446.3 cm^{-1}) at very high niobia loading (see Fig. 6).

Acidic properties of niobia/alumina. The IR spectra of pyridine adsorbed on niobia/alumina catalysts are presented in Fig. 3. The alumina support does not possess Brønsted acid sites, but contains strong Lewis acid sites (PyL band at 1449 cm^{-1}). The addition of niobia to the Al_2O_3 surface affects the characteristics of the Lewis acid sites and also creates new BAS at higher niobia loadings (see Figs. 3 and Table 1).

The concentration of the LAS increases with niobia loading to 5 wt% Nb_2O_5/Al_2O_3 and then decreases. This is due to concurrent and opposite processes: disappearance of Lewis Al sites and creation of Lewis Nb sites. Therefore, in order to estimate the lower limits for the second process, it is tentatively assumed that niobia is a neutral component of the niobia/alumina catalyst and that it does not contribute to the acidity. With this assumption it is possible to calculate the hypothetical amount of LAS originating only from the alumina support for each niobia/alumina catalyst. These hypothetical amounts of Lewis acid sites expressed in micromoles per gram of sample are as follows: 193 (199 × 0.97) for 3 wt% Nb_2O_5/Al_2O_3, 189 (199 × 0.95) for 5 wt% Nb_2O_5/Al_2O_3, 183 (199 × 0.92) for 8 wt% Nb_2O_5/Al_2O_3, 175 (199 × 0.88) for 12 wt% Nb_2O_5/Al_2O_5, and 161 (199 × 0.81) for 19 wt% Nb_2O_5/Al_2O_3. It is possible now to evaluate the excess Lewis acidity due to the amount of the deposited Nb atoms by taking the difference between the amount of LAS determined spectroscopically (from Table 1) and the hypothetical amount of LAS of the alumina support. Thus for the 3 wt% Nb_2O_5/Al_2O_3 catalyst the niobia contribution to the LAS equals 12.4%, for 5 wt% Nb_2O_5/Al_2O_3 catalyst it is 19.7%, and for 8 wt% Nb_2O_5/Al_2O_5 it is essentially equal 0% (0.2%). Consequently for 3 wt% Nb_2O_5/Al_2O_3 at least one out of eight Nb atoms contributes to Lewis acidity, for 5 wt% at least one out of five Nb atoms has its share in Lewis acidity, and for 8 wt% Nb_2O_5/Al_2O_3 there is still a very small contribution of Nb atoms to the number of LAS detected since the calculated values represent lower limits. For higher niobia loadings on alumina negative values for this Nb atomic contribution occur, and this means that for catalysts with higher niobia loading more Lewis acid sites disappear than are created by the addition of niobium oxide. It is also possible that these negative values of excess Lewis acidity stem from an overestimation of the hypothetical amounts of Lewis acid sites contributed by alumina at high loadings of niobia when the specific surface area of niobia/alumina catalysts is markedly decreased. The strength of the Lewis acid sites on niobia/alumina catalysts is relatively high (see Table 1 for thermodesorption data) and is a function of the LAS concentration (see Fig. 7). Interestingly, the same concentration-dependent pattern is also reflected in the behavior of the 1450 cm^{-1} PyL band (see Fig. 6). Eventually,

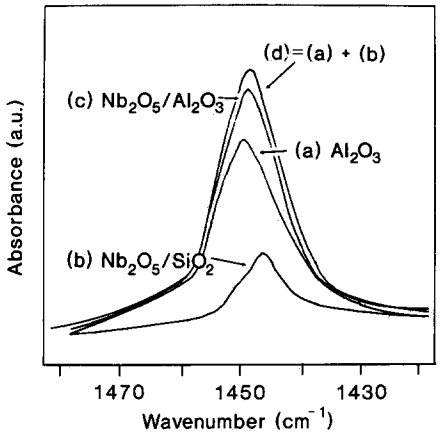

FIG. 8. Comparison of the 1450 cm^{-1} PyL band profiles in IR spectra of: (a) Al_2O_3, (b) 4 wt% Nb_2O_5/SiO_2 multiplied by 5/4 to correspond to 5 wt% Nb_2O_5/Al_2O_3, (c) 5 wt% Nb_2O_5/Al_2O_5, (d) sum of (a) and (b).

both the strength of LAS and the position of the 1450 cm^{-1} PyL band for the 19 wt% Nb_2O_5/Al_2O_5 catalyst approaches the value found for bulk niobia.

The hypothesis that the increase in the amount of Lewis acid sites upon deposition of low loadings of niobia on the alumina support originates from the combination of new Nb Lewis acid sites as well as already existing Al Lewis acid sites can be further confirmed from the IR spectra. Comparison of the 1450 cm^{-1} PyL band in the IR spectrum of pyridine adsorbed on 5 wt% niobia/alumina with the1450 cm^{-1} PyL band in the IR spectra of pyridine adsorbed on the alumina support and 4 wt% niobia/silica shows that the niobia/alumina PyL band is very similar to the linear combination of the PyL bands present in the IR spectra of the alumina and 4 wt% niobia/silica systems (see Fig. 8). This result supports the assumption that the 5 wt% niobia/alumina catalyst contains both Al Lewis acid sites (the same as in alumina) and Nb Lewis acid sites (the same as in the 4 wt% niobia/silica and plain niobia systems).

A similar approach can be applied in analyzing the nature of the decreased acid strength of Lewis sites in the niobia/alumina catalysts at high niobia contents. Figure 9 shows the IR PyL band for pyridine adsorbed on (a) alumina, (b) niobia (act. 200°C), (c) niobia/silica (the spectrum for 4 wt% niobia/silica has been multiplied by 19/4 to correspond to the 19 wt% niobia loading spectrum), and (d) 19 wt% niobia/alumina. The PyL band in the spectrum of pyridine adsorbed on the 19 wt% Nb_2O_5/Al_2O_3 catalyst appears very similar to the hypothetical spectrum of pyridine adsorbed on the 19 wt% Nb_2O_5/SiO_2, which indicates that the 19 wt% niobia/alumina catalyst possesses the same type of Lewis acid sites as the niobia and niobia/silica systems (i.e., Nb Lewis acid sites). The band characteristic of the Al Lewis acid sites is absent, suggesting that all Al Lewis acid sites have been substituted with Nb Lewis sites. The substitution of Al Lewis acid sites by weaker Nb Lewis acid sites explains the observed decrease of the acid strength of LAS in the niobia/alumina catalyst with increasing niobia content.

Brønsted acidity on niobia/alumina catalysts appears at higher niobia loadings (see Table 1). For the 8 wt% Nb_2O_5/Al_2O_3 catalyst only 1.7% of Nb atoms can be associated with the appearance of Brønsted acid

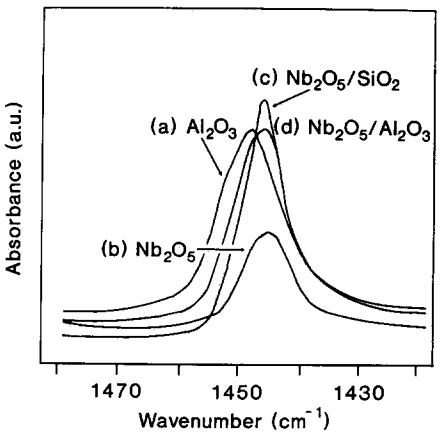

FIG. 9. Comparison of the 1450 cm^{-1} PyL band profiles in IR spectra of: (a) Al_2O_3, (b) Nb_2O_5, (c) 4 wt% Nb_2O_5/SiO_2 multiplied by 19/4 to correspond to 19 wt% Nb_2O_5/Al_2O_3, (d) 19 wt% Nb_2O_5/Al_2O_3.

sites. For the 12 and 19 wt% Nb_2O_5/Al_2O_3 catalysts the fraction of Nb atoms contributing to the Brønsted acid sites corresponds to the values 4.2 and 3.8%, respectively. It should be noted that the calculated amounts of BAS have been obtained by integrating the corresponding PyH^+ band and this procedure for this series of samples may result in an overestimation of these values by 5–10 μmol/g and produce an apparent discrepancy from a visual inspection of the PyH^+ band in Fig. 3.

Acidic properties of niobia/titania. The titania support (see Figs. 4 and 6) has some very weak Lewis acid sites. Their acid strength is lower than that in alumina and niobia ($A_{des}/A_0 = 0$, and lower frequency of the 1450 cm^{-1} PyL band). The deposition of niobia on titania (see Table 1 and Fig. 7) replaces weak Ti Lewis acid sites by only slightly stronger Nb Lewis acid sites (the frequency of PyL band shifts from 1444 cm^{-1} characteristic of Ti Lewis acid sites to only 1445 cm^{-1}, which is still below the value characteristic of Nb Lewis acid sites (Fig. 6)). The possible explanation is that for the 10 wt% Nb_2O_5/TiO_2 catalyst the amount of bulk-like niobia structures on the surface is still rather low. The decrease of the PyL band intensity with increasing niobia loading (Fig. 7) suggests that the Nb deposition removes more Ti Lewis acid sites than creates new Nb-sites. The same behavior was also observed in the niobia/alumina system for higher loading of niobia (Fig. 7). The rate of decrease in the amount of LAS, however, is smaller for the 10 wt% Nb_2O_5/TiO_2 catalyst than for the 5 wt% Nb_2O_5/TiO_2 catalyst (-7.4 and -12.2% with respect to the amount of Nb atoms, respectively).

Acidic properties of niobia/zirconia. The IR spectra of pyridine adsorbed on niobia/zirconia catalysts are shown in Fig. 5. The change in the LAS concentration upon deposition of niobia on zirconia as a function of niobia loading is presented in Table 1 and Fig. 7. The pure zirconia support, as well as niobia/zirconia catalysts, reveals essentially only Lewis acidity. The amount of LAS decreases with the amount of deposited Nb atoms, but the loss in LAS is more rapid at low niobia loadings. The loss in LAS with respect to the amount of deposited Nb atoms are -21.3% for the 1 wt% Nb_2O_5/ZrO_2, -11.7% for the 5 wt% Nb_2O_5/ZrO_2, and -4.1% for the 10 wt% Nb_2O_5/ZrO_2. The position of the 1450 cm^{-1} PyL band is initially at 1444 cm^{-1}, characteristic of the zirconia support, decreases to 1443 cm^{-1} for 5 wt% Nb_2O_5/ZrO_2, and then increases to 1446 cm^{-1} for 10 wt% Nb_2O_5/ZrO_2, which is characteristic of niobia. This behavior suggests that the LAS observed for the niobia/zirconia system are weaker at low niobia loadings (below a monolayer coverage) than with the LAS on bulk zirconia, but subsequently become stronger at high niobia loadings (above a monolayer coverage).

DISCUSSION

Molecular structures of surface niobium oxide overlayers. The supported niobium oxide catalysts investigated in this work span a broad range of niobia loadings, which correspond to below and above monolayer surface coverages. The evidence for surface niobium oxide overlayers on the oxide supports is provided by XPS analysis, XRD measurements, and Raman spectroscopy (15, 19). Below the monolayer coverage, the XPS studies reveal a linear relationship between the (Nb/Me) surface ratios and (Nb/Me) bulk ratios due to the formation of the two-dimensional niobium oxide overlayer. A departure from linearity at higher loadings suggests the transition from a two-dimensional niobia overlayer to three-dimensional crystalline phase. This finding is further confirmed by XRD and Raman spectroscopy measurements. Both of these analytical methods detect traces of crystalline Nb_2O_5 particles at approximately the same niobia loadings, and Raman spectroscopy also directly monitors the surface niobium oxide overlayer (15, 19). The collective application of these experimental techniques provides the following values for monolayer coverage in the different supported niobium

oxide catalysts: ~19 wt% in Nb_2O_5/Al_2O_3, ~7 wt% in Nb_2O_5/TiO_2, and ~5 wt% in Nb_2O_5/ZrO_2. Monolayer coverage is never achieved for the niobia/silica and niobia/magnesia systems because of the coexistance of crystalline niobia (niobia/silica) and bulk niobates (niobia/magnesia) almost from the very first steps of the niobia deposition.

Recent *in situ* Raman spectroscopy studies of the supported niobium oxide catalysts (*15, 19*) provide additional insights into the molecular structures present in these systems and, thus, also into the origin of Lewis and Brønsted acidity. It has been found that the surface niobia species present at low loadings of niobia on the alumina, titania, and zirconia supports are characterized by highly distorted NbO_6 octahedral units, while at higher niobia loadings the second type of the surface niobia species, with less distorted NbO_6 octahedral units, becomes predominant. A highly distorted NbO_6 octahedral structure has also been proposed for niobia deposited on the SiO_2 support for niobia loadings lower or equal to 2 wt%. The amount of surface niobia species in the niobia/silica and niobia/magnesia catalysts, as revealed by Raman measurements, appears to be very low. In fact, for the niobia/magnesia system the major components, even at very low niobia loading, are magnesium or calcium niobates rather than the surface niobia species; however, a small amount of these species can also be detected at higher niobia loadings. Similar bulk metal oxide compounds have also been found for the molybdena/magnesia and tungsta/magnesia systems (*22*).

Lewis acidity. The pyridine adsorption results for the Nb_2O_5/Al_2O_3 catalysts reveal that the new Nb Lewis acid sites appear on the Nb_2O_5/Al_2O_3 catalysts at low niobia loadings, achieve their maximum for the 5 wt% niobia/alumina sample, and then disappear at higher niobia loadings (see Fig. 7). However, the amount of LAS at the highest niobia loading of this study, which corresponds to monolayer coverage (19 wt% Nb_2O_5/Al_2O_5), is still very high and about 3 times greater than the value that would be expected for bulk niobia as the major component of the system above monolayer coverage. The above behavior seems to be directly related to the structural transformation of surface niobia species detected for this system in the Raman experiments. The amount of Lewis acid sites in the niobia/titania and niobia/zirconia catalysts decreases nonlinearly with niobia loading, which suggests that the new LAS are formed in these systems as well (see Fig. 7). A linear decrease of the LAS concentration with loading would mean that the LAS existing on the surface of the support disappear proportionally to the fraction of the surface occupied by the deposited niobia. In the case of the niobia/zirconia systems there is also a slight increase in Lewis acidity for niobia loading above monolayer coverage due to bulk Nb_2O_5 (see Fig. 7). Thus, at least to some degree, the Lewis acid sites present in these systems can be attributed to the surface niobium oxide phase on TiO_2 and ZrO_2. The direct estimation of the amount of Lewis acid sites from our IR pyridine adsorption data cannot be carried out here for the reasons previously discussed. The presence of the surface niobia/magnesia compounds in the case of the supported niobia/magnesia system and the bulk niobia phase in the case of niobia/silica system complicates such an evaluation since the Lewis acidity observed in the niobia/magnesia and niobia/silica series has its origin with these types of surface compounds or bulk metal oxide structures. It is possible, however, that in the case of the niobia/silica series of catalysts these surface structures also contribute, at least to some degree, to the Lewis acidity observed at very low loadings of niobia.

The appearance of Lewis acidity in binary mixed bulk metal oxide systems can be explained and predicted in many cases by the existing theoretical models (*23–25*), but very little is still known about the rules that govern this phenomenon for the surface

metal oxide species (i.e., supported niobium oxide catalysts). Recently, Connell and Dumesic (*26*) have proposed a model to explain the formation of Lewis acid sites for ions deposited on metal oxide supports. Their model, which is an extension of Tanabe's concept for diluted mixed binary bulk metal oxides, successfully explains the creation of Lewis acid sites for metal oxides doped with SiO_2 (*27*), but it is less effective for other systems. The model assumes that the formal charge on the deposited cation (in our case Nb^{+5}) is balanced by the coordinating surface lattice oxygen ions and that a cation is coordinatively undersaturated if it has a coordination number lower than that of Si ions in SiO_2. The authors also make an additional constraint about the matrix oxide, which requires that the supporting oxide must be free from strong basic oxygen anions. The application of the Connell and Dumesic model to the systems investigated in the present study leads to the following predictions about Lewis acidity: new Lewis acid sites should be created in the niobia/alumina, niobia/titania, and niobia/zirconia systems, and there should be no new Lewis acid sites due to the surface niobia species in the niobia/silica and niobia/magnesia catalysts. It should be noted that Tanabe's model gives essentially the same predictions except for the niobia/magnesia system for which the presence of Lewis acid sites is postulated. Both models have strictly local character, and neither of these approaches take into consideration the quantitative change in the number of acid sites with the increase of concentration (especially surface concentration) of the admixed minor component.

Comparison of our IR pyridine adsorption results with the theoretical model predictions for Lewis acid sites appears to be satisfactory. The appearance of LAS in the Nb_2O_5/Al_2O_3, Nb_2O_5/TiO_2, and Nb_2O_5/Al_2O_3 catalysts is in accordance with the expectations. A similar conclusion for the Nb_2O_5/SiO_2 and Nb_2O_5/MgO systems cannot be drawn for the above-cited reasons. Moreover, it should be stressed, once again, that the direct comparison of the LAS concentrational dependence with the theoretical predictions is simply unfeasible since none of the existing theories are able to provide such detailed estimations.

Additional information on the properties of the Lewis acid sites can be obtained from an analysis of their acid strength. The relative strength of the Lewis acid sites can be determined from the thermodesorption experiments and the position of the PyL band. The analysis of the thermodesorption data collected for our catalysts reveals that the strongest Lewis acid sites exist on the surface of niobia/alumina (see Table 1). Upon increasing the niobia loading the sites become weaker and eventually at monolayer coverage their strength approaches, within experimental error, the strength of LAS of bulk niobia. The second position in this ranking should be assigned to the niobia/silica system, since the other catalysts exhibit an A_{des}/A_0 ratio that equals zero and cannot be easily ranked. It is possible, however, to get some further insight into this classification by analyzing the dependence of the 1450 cm^{-1} PyL band position on the amount of the deposited Nb atoms (see Fig. 6). It appears that the highest frequency shift is reflected in the position of this band for the niobia/alumina catalysts and then the niobia/silica catalysts. The straight line in Fig. 6 represents the position of the 1450 cm^{-1} PyL band for pure niobia. Below this line are the 1450 cm^{-1} PyL band positions for the niobia/magnesia and niobia/titania catalysts, and at the very bottom of this figure are the band positions for the niobia/zirconia system. For higher niobia loadings all these "frequency curves" converge to the value characteristic of bulk niobia. Surprisingly, it also appears that the frequency curves resemble quite well the functional dependence established between the amount of the Lewis acid sites and the loading (Fig. 7), but this similarity may only be coincidental. The question as to

how the acid strength of surface acid sites changes with their concentration has not been yet addressed by any theoretical model.

The relationship between acid strength and the average electronegativity of the investigated metal oxide or metal ions of binary oxide systems is thought to be fairly well resolved in the literature (*27, 28*). However, correlations between the electronegativity of the cations and the strength of acid sites in many mixed oxides appear to be rather poor (*28*). Sanderson's electronegativity equalization method (29) is usually applied to calculate average electronegativities of metal oxides or in its modified version to evaluate the electronegativity of an atom in a molecule (*30*). This approach usually reproduces some trends that can be observed, but does not provide real and reliable data for solid metal oxides (*31*) and is mainly used because of its simplicity. The application of this method to our systems with Sanderson's electronegativity scale published in 1967 (*32*) results in the following dimensionless values for the average electronegativities of the metal oxides investigated in the present study: SiO_2 (2.751), Nb_2O_5 (2.507), Al_2O_3 (2.503), TiO_2 (2.383), ZrO_2 (2.289), and MgO (2.217). For pyridine the average electronegativity equals 2.433. From simple comparison of these values the conclusion can be made that silica should be the best candidate for the creation of strong Lewis acid sites, but that obviously is not true.

The above discrepancy can only be explained in terms of the theory proposed by Parr and Pearson (*33*). According to their theory, the coordinatively bonded complex between a pyridine molecule (electron donor) and a Lewis acid site (electron acceptor) should be the strongest if the fractional number of electrons transferred from the former to the latter is the greatest. This is in turn related to the ratio of the difference between the absolute electronegativities (Mulliken's definition) of both reaction partners to the doubled sum of the parameters defining their absolute hardness (the first derivative of the absolute electronegativity). Therefore, to have a strong interaction between a Lewis acid site and pyridine, not only the difference between the corresponding electronegativities must be positive (which corresponds to the thermodynamically favored situation with $\Delta G < 0$), but also the sum of their hardness parameters must be relatively low. The high absolute hardness of silica is probably the reason why Lewis acid sites cannot be detected by the chemisorption of pyridine. Unfortunately, there is still not enough data, especially for solid phases, to perform here more detailed estimations. Van Genechten and Mortier (*31*) have recently shown that the real values of the average electronegativity for different polymorphs of SiO_2 are actually greater than expected and depend upon the type of crystallographic structure.

Brønsted acidity. In the present study the Brønsted acidity has been found for two series of catalysts: niobia/silica and niobia/alumina. It has also been previously found that Brønsted acid sites appear on the surface of bulk niobium pentoxide (*21*). The theoretical predictions concerning the appearance of BAS in binary metal oxide systems can be obtained from the model considerations proposed by Tanabe *et al.* (*24*) and in the case of the silica support from the model proposed by Kataoka and Dumesic (*34*). The presence of BAS on the surface of the niobia/silica catalysts was essentially predicted in (*34*) for octahedral coordination of Nb atoms. Unfortunately, this prediction cannot be confirmed or discarded because the Brønsted acidity found for our niobia/silica samples at high niobia loadings (starting from above 4 wt%) originates from the bulk niobia phase rather than the surface niobia species. Surface Brønsted acidity of this type has been found, however, for the niobia/alumina system. It also begins at high surface coverages of niobia (from 8 wt% up). The appearance of Brønsted acidity in this system is in contrast to the predictions of Tanabe's model, which by its very nature is

unable to give the right answer. Predicting correctly the appearance of LAS, the model eliminates at the same time the appearance of BAS. In other words, Tanabe's model never predicts the simultaneous appearance of both types of acidity. For all the other supported niobium oxide catalysts investigated in this work only some traces of Brønsted acidity have been detected at very high niobia loadings, which correspond to small Nb_2O_5 particles present above monolayer coverage. The absence of BAS for niobia/titania and niobia/zirconia is consistent with the predictions obtained from the theoretical model proposed by Tanabe.

The "creation of new Brønsted acid sites" means that some new hydroxyls are formed upon supporting niobia on alumina or that some hydroxyls already existing on niobia or alumina become sufficiently acidic to protonate pyridine. The quantum-mechanical calculations carried out by Bernholc *et al.* (*12*) show that the alumina support lowers the proton removal energy of W–OH, Nb–OH, and Ti–OH by stabilization of the negatively charged state obtained by abstraction of the proton. This might be an argument in favor of the supported metal oxide origin of Brønsted acidity. Nevertheless, if this were the case the increase of the amount of BAS should already begin at low surface niobium oxide coverages, since there is enough supporting metal oxide to perform this stabilization function. Therefore, such an explanation for the origin of Brønsted acidity can be eliminated. The possibility that the support hydroxyls become acidic enough to protonate pyridine by the interaction with the supported metal oxide can also be discarded since nothing should happen to these hydroxyls upon exposure to a reducing atmosphere. Yet, the experiments with pyridine chemisorption performed for MoO_3/Al_2O_3 (*35, 36*) or MoO_3/TiO_2 (*37*) show that upon reduction the Brønsted acidity is completely suppressed.

The appearance of the new Brønsted acid sites can be explained by an interpretation based on model cluster calculations of the charges on protons and the proton abstraction energies for hydroxyl groups in zeolites (*38, 39*). This interpretation assumes, when referred to our case, that the creation of Brønsted acid sites requires both Al and Nb atoms. The Brønsted acid sites are bridging hydroxyl groups, Al–OH–Nb. The results of the model cluster calculations for zeolites show that Al–OH–Si bridging hydroxyls possess higher positive charges and lower proton abstraction energies than those of Si–OH or Al–OH, which makes the bridging hydroxyls more acidic. In addition, it has been shown that these effects are stronger if there are more Si tetrahedra than Al tetrahedra in the second coordination shell with respect to the Al–OH–Si bridging hydroxyl (*39*). That refers only to Si atoms because Al tetrahedra in zeolites are never neighbors to each other (Løwenstein's exclusion rule). This implies that Al–OH–Nb bridging hydroxyls should be more acidic when there are more Nb atoms in the vicinity of the Nb atom in the bridging group. The above conclusion is consistent with our pyridine adsorption experiments, which reveal that a critical concentration of surface niobia species is required to create the BAS (to make the bridging hydroxyls acidic with respect to pyridine). The bridging structures are broken upon reduction and that accounts for the loss of Brønsted acidity. The appearance of BAS coincides with the structural transformation of surface niobia species, which takes place at higher niobia loadings and that has been revealed by Raman measurements (*19*). The possibility that the bridging hydroxyls may be created between the Nb atoms belonging to different niobia layers cannot be excluded, but the elucidation of this problem will require more data from additional quantum-mechanical model cluster calculations of such layered structures.

The CO_2 adsorption experiments performed for the niobia/alumina system reveal that there are almost no absorption bands for CO_2 chemisorbed on the surface of the 19 wt% Nb_2O_5/Al_2O_3 catalyst (*13*). Since it

has been proven by Tanabe and co-workers (*21*) that plain niobia has no basic hydroxyls, this suggests that basic hydroxyls are not left on the alumina surface and that the support is completely covered by the surface niobium oxide overlayer. It is possible, however, that there are still some exposed patches of the alumina surface free from basic hydroxyls, but with enough Al Lewis acid sites to account for the observed high Lewis acidity. Of course, it could also mean that for catalysts with niobia loading below approximately 8 wt% there are one-layered niobia structures and above this value multilayered niobia structures of niobium oxide on the surface of the supporting oxide. Probably, this is the structural change that is reflected in the *in situ* Raman spectra of the niobia/alumina system. Such structural changes could also explain the appearance of the Brønsted acidity generated by these unique multilayered NbO_6 octahedral units of the alumina-supported niobium oxide at high niobia loadings (above $\sim\frac{1}{2}$ monolayer). The absence of these multilayered surface niobia clusters on the other supports investigated in this study could account for the absence of the related Brønsted acid sites (the bridging Nb–OH–Al fragments in one-layered niobia clusters are not acidic enough to protonate pyridine).

CONCLUSIONS

The IR spectra of chemisorbed pyridine reveal Lewis acidity in all the investigated catalysts composed of niobia supported on silica, magnesia, alumina, titania, and zirconia. The observed Lewis acidity can be associated not only with the LAS already existing on a support, but also with the surface niobium oxide species (with the exception of the niobia/magnesia and niobia/silica systems). The resulting Lewis acid sites are usually weaker than the Lewis acid sites initially present on the oxide supports. The presence of the new Lewis acid sites can be explained in terms of local coordinative unsaturation of the dopant Nb cations due to specific interactions between the cations and the support. The general predictions from the models that apply Pauling's electrostatic bonding rules (*24, 26, 27*) have been experimentally confirmed, but no theoretical explanation for the surface coverage dependence of the Lewis acidity found for the supported niobium oxide catalysts currently exists. At monolayer coverage, however, the acidic characteristics of the Lewis acid sites approach the acidic properties of the Lewis acid sites of bulk niobium oxide. The relationship between the loading of the supported metal oxide and the LAS acid strength is also not addressed by these theories.

Significant concentrations of Brønsted acid sites are only present for two systems (niobia/silica and niobia/alumina), but only in the latter case are they due to the surface niobia species. Brønsted acidity appears at a critical surface coverage of the supported niobium oxide species ($\sim\frac{1}{2}$ monolayer), increases linearly with further increase in surface coverage, and achieves its maximum before monolayer coverage. There is a direct relationship between the critical concentration and the structural transformation of the surface metal oxide species. The Brønsted acidity is most probably associated with the creation of bridging hydroxyls formed between the surface niobium oxide species and the alumina support. None of the existing theories predict Brønsted acidity in the niobia/alumina system and or address the problem of its specific behavior upon increasing the surface niobium oxide coverage.

ACKNOWLEDGMENTS

The authors thank Dr. R. P. Eischens for allowing us to use his FTIR instrumental setup and Niobium Products Company for their financial support.

REFERENCES

1. Parry, E. P., *J. Catal.* **2,** 371 (1963).
2. Knozinger, H., *in* "Advances in Catalysis" (D. D. Eley, H. Pines, and P. B. Weisz, Eds.), Vol. 25, p. 184. Academic Press, New York, 1976.
3. Dollish, F. R., Fately, W. G., and Bentley, F. F., "Characteristic Raman Frequencies of Organic Compounds." Wiley, New York, 1974.

4. Kung, M. C., and Kung, H. H., *Catal. Rev.-Sci. Eng.* **27,** 425 (1985).
5. Hughes, T. R., and White, H. M., *J. Phys. Chem.* **69,** 2192 (1965).
6. Ward, J. W., *J. Catal.* **34,** 10 (1968).
7. Ward, J. W., *J. Colloid Interface Sci.* **28,** 269 (1968).
8. Datka, J., and Piwowarska, Z., *J. Chem. Soc. Faraday Trans. 1* **85,** 47 (1989).
9. Murrell, L. L., Grenoble, D. C., and Kim, C. J., US Patent 4,233,139 (1980).
10. Murrell, L. L., and Grenoble, D. C., US Patent 4,415,480 (1983).
11. Okazaki, S., and Okuyama, T., *Bull. Chem. Soc. Jpn.* **56,** 2159 (1983).
12. Bernholc, J., Horsley, J. A., Murrell, L. L., Sherman, L. G., and Soled, S., *J. Phys. Chem.* **91,** 1526 (1987).
13. (a) Jehng, J. M., and Wachs, I. E., *Prepr. Am. Chem. Soc. Petrol. Chem. Div.* **34,** 546 (1989); (b) *in* "Novel Materials in Heterogeneous Catalysis" (R. T. Baker and L. L. Murrell, Eds.), p. 232. American Chemical Society, Washington, DC, 1990).
14. Wachs, I. E., Jehng, J. M., and Hardcastle, F. D., *Solid State Ionics* **32/33,** 904 (1989).
15. Jehng, J. M., and Wachs, I. E., *Catal. Today* **8,** 37 (1990).
16. Asakura, K., and Iwasawa, Y., *Chem. Lett.,* 511 (1986).
17. Asakura, K., and Iwasawa, Y., *Chem. Lett.,* 633 (1988).
18. Nishimura, Y., Tanaka, T., Kanai, H., Funabiki, T., and Yoshida, S., *Catal. Today* **8,** 67 (1990).
19. (a) Jehng, J. M., and Wachs, I. E., *J. Mol. Catal.* **67,** 369 (1991); (b) *J. Phys. Chem.* **95,** 7373 (1991); (c) Jehng, J. M., Ph.D. thesis, Lehigh University, 1990.
20. Datka, J., *J. Chem. Soc. Faraday Trans. 1* **77,** 2877 (1981).
21. Iizuka, T., Ogasawara, K., and Tanabe, K., *Bull. Chem. Soc. Jpn.* **56,** 2927 (1983).
22. Williams, C., Ekerdt, J., Jehng, J. M., Hardcastle, F. D., and Wachs, I. E., submitted for publication.
23. Thomas, C. L., *Ind. Eng. Chem.* **41,** 2654 (1949).
24. Tanabe, K., Sumiyoshi, T., Shibata, K., Kiyoura, T., and Kitagawa, J., *Bull. Chem. Soc. Jpn.* **47,** 1064 (1974).
25. Kung, H., *J. Solid State Chem.* **52,** 191 (1984).
26. Connell, G., and Dumesic, J. A., *J. Catal.* **102,** 216 (1986).
27. Connell, G., and Dumesic, J. A., *J. Catal.* **105,** 285 (1987).
28. Shibata, K., Kiyoura, T., Kitagawa, J., Sumiyoshi, T., and Tanabe, K., *Bull. Chem. Soc. Jpn.* **46,** 2985 (1973).
29. Sanderson, R. T., "Chemical Bonds and Bond Energy." Academic Press, New York, 1976.
30. Craver, J. C., Gray, R. C., and Hercules, D. M., *J. Am. Chem. Soc.* **96,** 6851 (1974).
31. Van Genechten, K. A., and Mortier, W. J., *J. Chem. Phys.* **86,** 5063 (1987).
32. Sanderson, R. T., "Inorganic Chemistry." pp. 72–76. Van Nostrand–Reinhold, New York, 1967.
33. Parr, R. G., and Pearson, R. G., *J. Am. Chem. Soc.* **106,** 7512 (1983).
34. Kataoka, and Dumesic, J. A., *J. Catal.* **112,** 66 (1988).
35. Segawa, K., and Hall, W. K., *J. Catal.* **76,** 133 (1982).
36. Suarez, W., Dumesic, J. A., and Hill, C. G., *J. Catal.* **94,** 408 (1985).
37. Kim, D. S., Ph.D. thesis, Sophia University, Tokyo, 1989.
38. Mortier, W. J., Sauer, J., Lercher, J. A., and Noller, H., *J. Phys. Chem.* **88,** 905 (1984).
39. Kazanskii, V. B., *Kinet. Catal.* **23,** 1131 (1982).